Applied Catalysis B: Environmental 172–173 (2015) 129–135

Contents lists available at ScienceDirect

Applied Catalysis B: Environmental

journal homepage: www.elsevier.com/locate/apcatb

Low temperature H_2 production from ammonia using ruthenium-based catalysts: Synergetic effect of promoter and support

Alfred K. Hill, Laura Torrente-Murciano *

Department of Chemical Engineering and Centre for Sustainable Chemical Technologies, University of Bath, Bath BA27AY, UK

ARTICLE INFO

Article history:
Received 6 November 2014
Received in revised form 21 January 2015
Accepted 10 February 2015
Available online 11 February 2015

Keywords:
Ammonia decomposition
In-situ H_2 production
Low temperature activation
Ruthenium
Promoters

ABSTRACT

Low temperature hydrogen production via ammonia decomposition is achieved by the synergetic combination of a highly conductive support and an electron donating promoter in a ruthenium-based system, with activity at temperatures as low as 450 K. The high conductivity of graphitized carbon nanotubes allows for greater electronic modification of the ruthenium nanoparticles by cesium located in close proximity but without direct contact, avoiding the blockage of the active sites. This development of low temperature catalytic activity represents a breakthrough toward the use of ammonia as chemical storage for in-situ hydrogen production in fuel cells.

1. Introduction

Environmental concerns regarding the detrimental effects of anthropogenic CO_2 emissions into the atmosphere are increasingly leading the scientific community to the development of sustainable alternative fuels [1]. Hydrogen has long been considered as a suitable alternative as a carbon-free road transport fuel for high energy efficient proton exchange membrane fuel cells (PEM-FC), however, efforts to achieve a sufficient hydrogen storage density remain well short of the targets set by the US Department of Energy (DoE) for feasible safe portable systems [2]. With a hydrogen storage capacity at moderate pressure (<10 bar) that exceeds liquid hydrogen [3], ammonia's potential as a hydrogen vector is currently limited by the lack of a catalytic system capable of releasing hydrogen on-demand at temperatures aligned with those of the PEM-FC (~370 K).

The development and optimization of ammonia synthesis in the so-called Haber-Bosch process for more than 150 years has provided the foundations of the current efforts for the development of catalytic systems for the decomposition of ammonia [4]. Despite the reversibility of the reaction, new challenges arise in the decomposition path, especially at low reaction temperatures (<600 K) due to the low thermodynamic equilibrium conversions and the recombinative desorption of nitrogen adatoms as the rate determining step [5]. Engineering solutions such as membrane systems [6] can successfully integrate hydrogen production and in-situ separation maximizing ammonia utilization and avoiding poisoning of the fuel cell catalysts. This leaves the development of a low temperature catalytic system as the key challenge to unveiling ammonia as an energy vector toward the so-called hydrogen economy.

Despite considerable progress in the field, current catalytic systems can only achieve significant ammonia decomposition conversion at temperatures around 600 K [7] and consequently, its potential for on-demand hydrogen production at low temperatures has been disregarded. The only few previous studies of low temperature ammonia decomposition in the literature [8,9] suggest the feasibility of the system using ruthenium-based catalysts and their catalytic enhancement by the use of electron donating promoters such as cesium or potassium. We have recently demonstrated that optimization of the Ru/Cs ratio on Ru/CNT systems facilitates the production of hydrogen from ammonia at low temperatures. The activation energy is reduced via electronic modification of the active sites which facilitate the nitrogen recombinative desorption on the ruthenium surface [10]. In this work, we show the extraordinary enhanced activity of promoted ruthenium nanoparticles supported on graphitized carbon nanotubes (CNT) at temperatures as low as 450 K, revealing new insights into the synergetic effect of the promoter and a highly conductive support on the electronic modification of the ruthenium sites.

* Corresponding author: Tel.: +44 1225 38 5857; fax: +44 1225 38 5713.
E-mail address: ltm20@bath.ac.uk (A.K. Hill).

http://dx.doi.org/10.1016/j.apcatb.2015.02.011

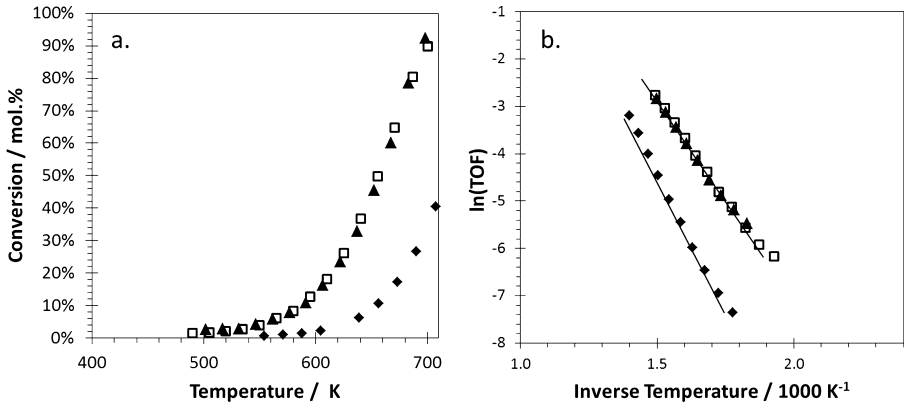

Fig. 1. (a) Ammonia decomposition conversion as a function of reaction temperature showing the effect of graphitization of the CNT support in un-promoted Ru catalysts (b) Arrhenius' plot (♦) 7 wt% Ru/CNT, (□) 7 wt% Ru/graphitized-CNT at 2073 K and (▲) 7 wt% Ru/graphitized-CNT at 2273 K Reaction conditions are detailed in the experimental section.

2. Experimental procedure

Multi-walled carbon nanotubes (Sigma Aldrich, OD 6–9 nm, length 5 μm, S_{BET} 253.0 $m^2\,g^{-1}$) were graphitized at 2070 and 2270 K during 1 h in an ultra-high vacuum furnace. All catalysts were synthesised by incipient wetness impregnation using $Ru(NO)(NO_3)_3$ (Alfa Aesar) and $CsOH.xH_2O$ (Sigma Aldrich, $x = 0.17$) as ruthenium and cesium precursors. After impregnation of the aqueous solutions, the catalysts were dried at 350 K under vacuum for 3 h and then reduced under hydrogen at 500 K for 1.5 h. Nitrogen adsorption analyses were carried out at 77 K using a Micromeritics ASAP 2020 instrument. The surface area was calculated using the Brunauer, Emmett and Teeler (BET) method. Ruthenium particle size distribution was estimated by microscopy using a JEOL TEM-2100 200 kV ultra-high resolution transmission electron microscope. Samples were prepared by dispersing the samples in ethanol (0.5 mg mL^{-1}). A drop of the dispersion was added to a Lacey carbon-coated copper mesh grid and dried under vacuum. CO pulse chemisorption analyses were carried out at 310 K using a Micromeritics Autochem II instrument equipped with a thermal conductivity detector (TCD). Samples were pre-treated for one hour at 525 K under helium flow to desorb water or any other impurity from the catalyst surface. Temperature programme reduction (TPR) experiments were carried out in the same equipment. In this case, the samples were degassed at 775 K under flowing Argon for 20 min prior to TPR analyses up to 1275 K using a temperature ramp rate of 10 K min^{-1} under 30 mL min^{-1} flow of 5% H_2/Ar. Raman analyses were carried out using a Renishaw in Via Raman microscope using a 532 nm green Renishaw Diode Laser.

Ammonia decomposition reactions were carried out in a continuous packed bed reactor with a gas hourly space velocity of 5200 $ml_{NH3}\cdot g_{cat}^{-1}\cdot h^{-1}$ using 25 mg of catalyst in a silica bed. The reactor system was equipped with mass flow and temperature controllers. All the pipes were heated to 333 K to avoid any ammonia condensation and consequently corrosion. During each catalytic study, the reaction temperature was ramped from around 450 K to 850 K at 2.6 K min^{-1} using a Carbolyte tubular furnace with PID control. Reactor exit gas was analysed using an on-line gas chromatography fitted with a Hayesep Q column and thermal conductivity detector. The mass balance closure precision was within a ±10% error.

3. Results and discussion

Graphitization of commercial multi-walled carbon nanotubes (CNT) substantially increases the ammonia decomposition conversion of unpromoted ruthenium catalysts while decreasing the minimum temperature of activation by ~100 K (Fig. 1a). The turnover frequency values at 600 K are an order of magnitude higher in the case of the graphitized catalysts with a substantial decrease in activation energy from 96.7 to 67.6 kJ mol^{-1} for the commercial and graphitized CNTs support, respectively, (Fig. 1b). None of the supports show any measurable conversion in the absence of ruthenium.

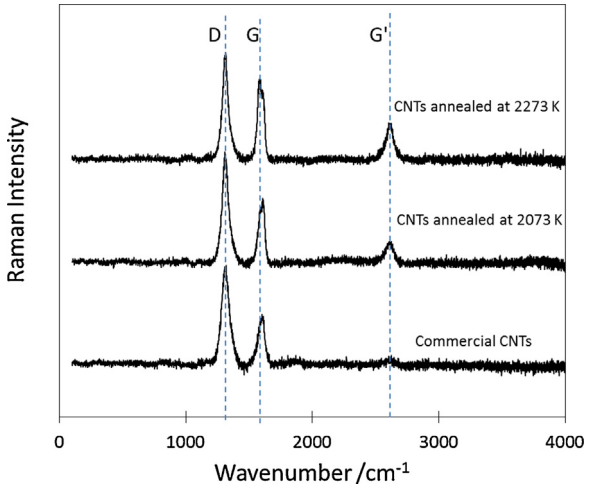

Fig. 2. Raman spectra of commercial multi-walled CNT and after graphitisation at 2073 and 2273 K under vacuum.

Annealing of the CNT at 2070 K and 2273 K under ultra-high vacuum modifies the chemical and physical surface properties of the support, increasing the axial alignment of the tubes and increasing the crystallite size [11], shown by a variation of the relative intensity of the peaks in the Raman spectra (Fig. 2).

The D band at 1350 cm^{-1} is representative of the disorder in graphitic carbon and the G and G' bands at 1580 cm^{-1} and 2700 cm^{-1} are produced by graphitic in-plane vibrations from sp^2-bonded carbon and 2D vibrations respectively and its prominence reflects the presence of graphitic carbon [12]. The lower I_D/I_G ratio of the annealed CNT with respect to the commercial ones suggests a more graphitic structure after the thermal treatment as shown in Table 1.

Graphitization is accompanied by the removal of any potential presence of residual iron catalyst remaining from the CNT's synthesis [11] and defects in the graphitic walls of the material. This healing of the CNT surface has a minor detrimental effect on the surface area of the material (Table 1) however it strongly promotes the elimination of functional groups on the CNT's surface [11]. Chemical

Table 1
Effect of graphitization at 2070 K on the CNT's physical properties.

Support	Surface area[a] $m^2\ g^{-1}$	Pore diameter[b] nm	Raman intensity I_D/I_G
Commercial CNT	253	27.6	2.6
Graphitised CNT @2070 K	220	28.4	1.9
Graphitised CNT @2270 K	235	28.0	1.5

[a] Calculated via N_2 physisorption at 77 K using BET equation.
[b] Using the BJH desorption data.

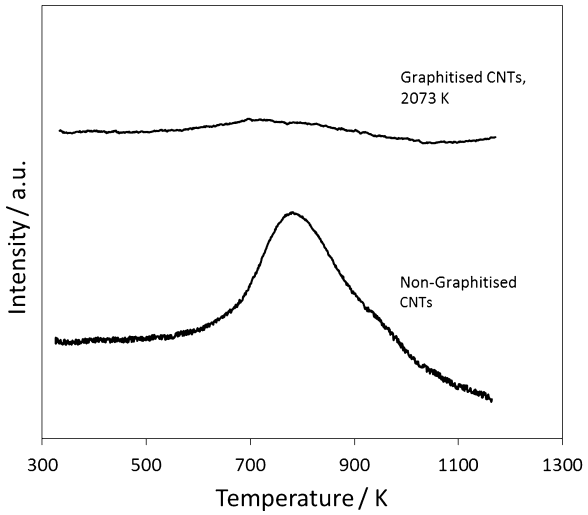

Fig. 3. Temperature programmed reduction (TPR) of commercial multi-walled CNT and after graphitisation at 2070 K under vacuum.

functionalization by acid oxidation and the introduction of phenolic, carboxyl, and lactone groups is common practice during the purification stages in the CNT's synthesis [13]. In general, these oxygen surface complexes are known to be thermally unstable and their removal during the graphitization process is here verified by temperature programmed reduction characterization (Fig. 3). While reduction of surface oxygen complexes is observed between 670 and 1270 K in the commercial CNT, negligible hydrogen consumption is observed in the annealed sample as expected due to the lack of such groups in its surface, verifying its graphitization.

Functional surface groups and defects on carbon materials are known to act as anchoring points for the metal active nanoparticles, improving their dispersion across the surface [14] which are mostly removed during graphitization. In any case, ruthenium particles present similar size distribution when supported on commercial CNT and graphitized CNT (Fig. 4). The surface area of the Ru-supported catalysts does not significantly vary respect to their respective supports. Other authors have previously claimed that metal nanoparticles might tend to locate more preferentially on the outer surface of the graphitized CNT due their higher degree of order compared to the inner walls [15] but we do not have a clear evidence of this phenomena. Unfortunately, XRD spectra of these catalysts do not provide useful information related the average crystallite size of the ruthenium particles due to the overlap of the ruthenium and support diffraction peaks.

Instead, the activity enhancement is believed to be caused by an increase of the CNT's electron conductivity during graphitization which consequently modifies the metal-support interaction. The defects and functional groups on the surface of CNT reduce the effective band overlap of the support, leading to an increase in the electrical resistivity [16]. Their removal during graphitization has been shown to greatly increase the material's conductivity [17]. According to that study, the CNT's conductivity increases exponentially with the graphitization temperature below 1770 K. Further increments in the annealing temperature only lead to small incremental enhancements of the conductivity. Indeed, similar catalytic activity toward ammonia decomposition is observed with 7 wt% ruthenium catalysts supported on graphitized CNT at 2070 and 2270 K, respectively, (Fig. 1). Graphitization results in a higher electron density in the CNT's outside walls and a high conductivity which facilitates the electron transfer between the support and the ruthenium particles promoting the recombination of nitrogen, making the catalytic system active at lower temperatures.

Interestingly, a similar modification of the ruthenium sites achieved by graphitization of the CNT support is observed by the addition of 4 wt% cesium as electron donating promoter to the non-graphitized catalysts (Fig. 5, solid triangles and solid line, respectively), with a similar activation energy. Thus, we further investigated the combined effect of cesium loading and the use of graphitized CNT in the modification of the ruthenium activity.

Fig. 5 shows a remarkable synergetic effect of the combination of cesium to ruthenium sites supported on graphitized CNT's. 7 wt% Ru-4 wt% Cs/graphitized CNT presents activity toward decomposition at temperatures as low as 450 K, with a respective decrease of the activation energy as shown in Table 1. However, surprinsingly, higher cesium loadings does not further enhance the catalytic activity neither decreases the minimum temperature of activity, as previously observed for the Ru-based catalysts on commercial CNT [10].

The variations on the catalytic activity of Cs-promoted ruthenium catalysts supported on graphitized CNT are not caused by relevant variations on the ruthenium particle size distribution as shown by representative TEM pictures in Fig. 6. Although the particle size distribution seems to be shifted toward bigger particles as the cesium loading increases, the differences (<1 nm) are within the experimental error associated to TEM particle sizing despite care been taken in imaging multiple locations within each sample. The cesium loading does not either seem to have an effect on the preferential distribution of the ruthenium nanoparticles in the inside or outside surface of the carbon nanotubes. Indeed, in Fig. 6 we have intentionally shown pictures were most of the ruthenium nanoparticles are situated inside and outside the CNT's to demonstrate the lack of a systematic trend. It is important to note that cesium is not detectable by TEM even at the high loadings used herein.

The similitude on ruthenium particle size in the Cs-promoted ruthenium supported on graphitized CNT observed by TEM is not in agreement with the exposed metallic surface areas measured by CO chemisorption (Table 2). This disagreement suggest the partial coverage of the ruthenium sites by cesium, especially at high Cs loadings, blocking the CO access during the CO chemisorption analysis. Considering this, the Cs/Ru molar ratio is expected to have an effect in this phenomena. Indeed, Fig. 7 shows a sharp increase in the ammonia decomposition rate of reaction by the addition of cesium which reaches a maximum activity at a Cs/Ru molar ratio of 0.6, above which the activity decreases.

The addition of cesium has a double effect on the catalytic activity of ruthenium-based catalysts. On one hand, cesium located on the surface of ruthenium or its close proximity produces a beneficial electronic modification of the ruthenium, responsible of the ammonia decomposition catalytic activity enhancement. On the

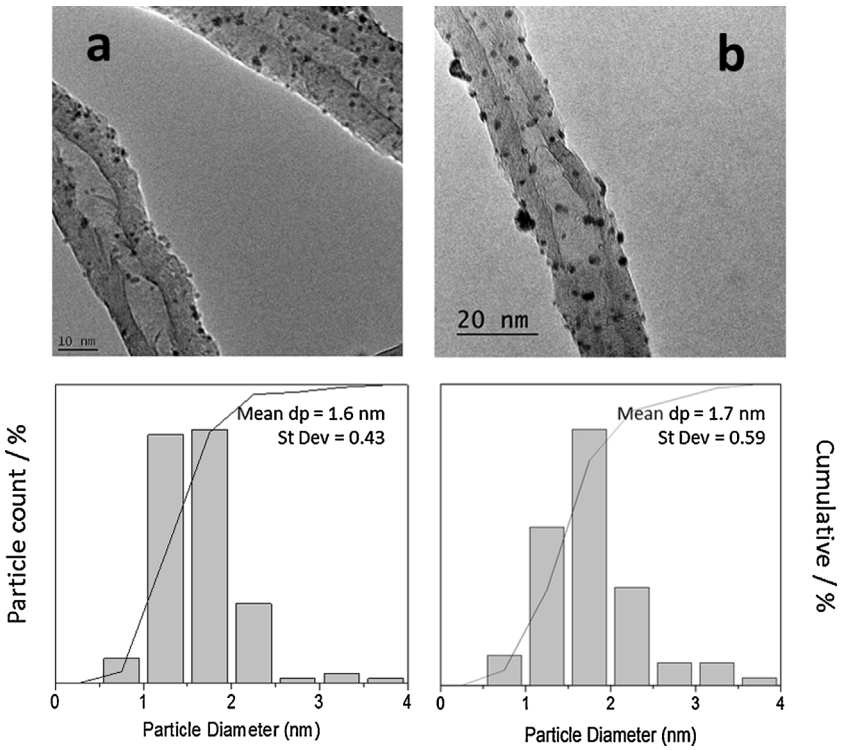

Fig. 4. TEM images and particle size histograms of 7 wt% Ru/CNT catalysts (a) Commercial CNT and (b) Graphitised CNT at 2070 K. Particle size distributions are calculated from different locations measuring between ~100 nanoparticles.

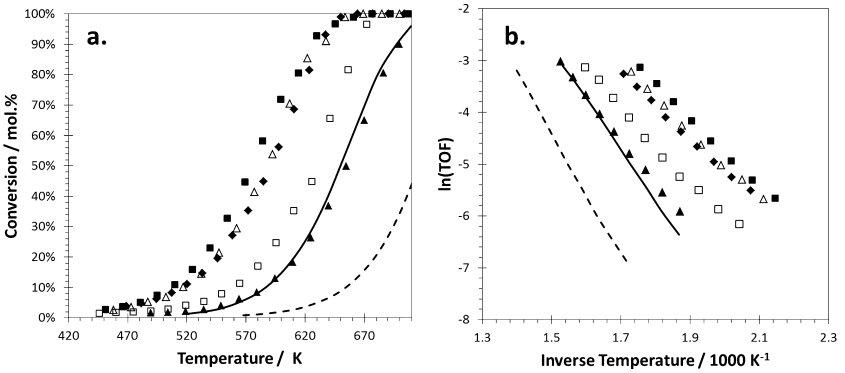

Fig. 5. (a) Ammonia decomposition conversion as a function of reaction temperature showing the synergetic effect of graphitization of the CNT support and addition of Cs promoter in Ru catalysts (b) Arrhenius' plot (▲) 7 wt% Ru/graphitized CNT, (■) 7 wt% Ru 4 wt% Cs/graphitized CNT, (Δ) 7 wt% Ru 10 wt% Cs/graphitized CNT, (♦) 7 wt% Ru 20 wt% Cs/graphitized CNT and (□) 7 wt% Ru 30 wt% Cs/graphitized CNT. Dashed line: 7 wt% Ru/CNT and solid line: 7 wt% Ru 4 wt% Cs/CNT for comparison. Reaction conditions are detailed in the experimental section.

Table 2
Effect of CNT's graphitization and cesium loading on 7 wt% Ru/CNT catalysts for the decomposition of ammonia reaction.

Support	Cesium loading/wt%	Cs/Ru ratio	Ru average particle size[a]/nm	CO adsorbtion[b]/mol CO g^{-1}	TOF @600 K[c]/mol_{NH3} $mol^{-1}{}_{Ru}$ h^{-1}	Activation energy/kJ mol^{-1}
Commercial CNT	0	–	1.6	3.0	6.5	96.7
Commercial CNT	4	0.6	1.6	2.8	41.4	78.6
Commercial CNT	20	2.8	2.0	2.8	154.4	59.3
Graphitized CNT	0	–	1.6	2.3	48.9	67.6
Graphitized CNT	4	0.6	1.7	2.2	242.3	53.5
Graphitized CNT	10	1.4	2.1	3.0	207.0	49.5
Graphitized CNT	20	2.8	2.4	1.1	176.4	49.6
Graphitized CNT	30	4.6	2.6	1.4	122.4	61.7

[a] Average particle size determined by TEM.
[b] CO chemisorption at 310 K.
[c] Reaction conditions are detailed in the experimental section.

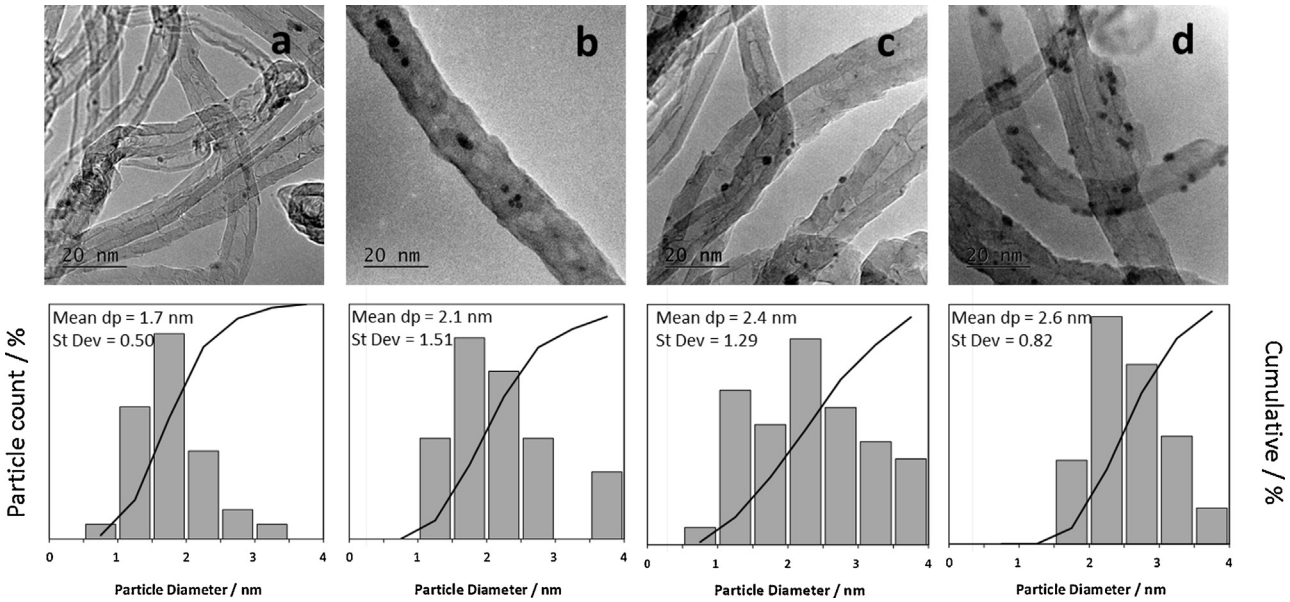

Fig. 6. TEM images and particle size histograms of Cs-promoted 7 wt% Ru/graphitized CNT catalysts (a) 4 wt% Cs, (b) 10 wt% Cs, (c) 20 wt% Cs and (d) 30 wt% Cs. Particle size distributions are calculated from different locations measuring between ~100 nanoparticles.

other hand, cesium located on the surface of ruthenium blocks the access of ammonia to the ruthenium active sites, having a detrimental effect on the overall activity. The volcano curve on the effect of cesium loading on the reaction rate is the manifestation of this double effect (Fig. 7).

The different optimum Cs/Ru molar ratio of the CNT and the graphitized CNT supports offers insights about the actual role of promoter, support and their synergetic effect. Although graphitization of the CNT is likely to modify the relative heat of adsorption of the promoter on the ruthenium and the support surface, cesium does not seem to preferentially adsorb on the ruthenium surface on the graphitized CNT catalysts compared to the same catalyst with the commercial CNT support as suggested by CO chemisorption analyses (Table 2). Similar amounts of CO are chemisorbed in all the catalytic systems, with graphitized and commercial CNT supports, suggesting a similar exposure of ruthenium metallic surface. The differences are related to the slight variations in ruthenium particles size and the coverage of the ruthenium nanoparticles by cesium, especially at high cesium loadings (>20 wt%) [10].

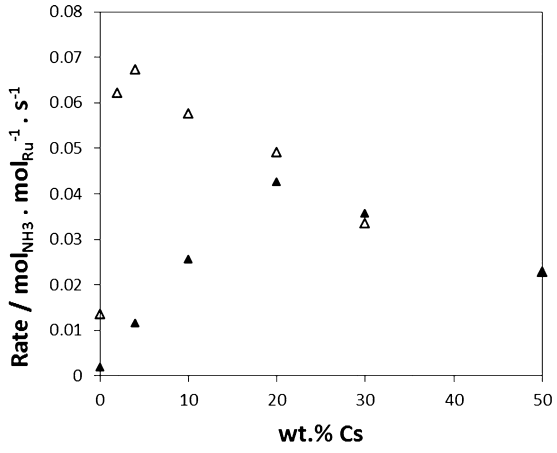

Fig. 7. Effect of cesium loading on the ammonia decomposition rate of reaction at 600 K using 7 wt% Ru/CNT catalysts (▲) Commercial CNT (△) graphitized-CNT at 2070 K. Reaction conditions are detailed in the experimental section.

The degree of electronic modification of ruthenium by the presence of cesium can be elucidated by temperature programmed reduction analyses (Fig. 8). Ruthenium particles present the same reduction temperature at ~440 K when supported in both commercial and graphitized CNT in the absence of cesium which suggests similitudes on particle size and metal-support interaction. The reduction temperature and integrated area of this peak (values on Table 3) increase as the cesium loading increases due to the simultaneous reduction of the ruthenium and the cesium located on its surface [10].

The shift of the ruthenium reduction temperature as the cesium loading increases suggests the simultaneous electronic modification of both elements when in contact to each other. While cesium-only supported on CNT does not reduce below ~600 K, the ruthenium's capability of dissociating hydrogen [18] allows the reduction of cesium on direct contact with ruthenium at considerably lower temperatures [10]. Graphitization of the CNT support facilitates the hydrogen spillover to the surrounding area, allowing the reduction of cesium in the ruthenium proximity which is speculated to correspond to the reduction peak ~380 K. In this way, ruthenium supported on graphitized CNT is electronically modified simultaneously by the cesium located in its surface and the cesium located in its close proximity.

The high electron conductivity of the graphitized CNT reciprocally allows the electronic modification of the ruthenium sites by the cesium situated by this wide surrounding area (distance modification), developing activity at lower reaction temperatures. This promotional effect results in a higher electron density in the ruthenium particles reflected in lower activation energy of 53.5 kJ mol^{-1} compared to the 78.6 kJ mol^{-1} achieved with the equivalent Ru-Cs system in commercial CNT (Cs/Ru molar ratio of 0.6).

An increase of the Cs/Ru ratio decreases the number of ruthenium active sites accessible to the reaction due to cesium deposition on its surface, which is reflected in a decrease of the amount of CO chemisorbed (Table 2). While this is beneficial in the commercial CNT catalyst as only the cesium located in the ruthenium surface has a promotional effect, small amounts of cesium are enough to achieve the necessary electronic modification of ruthenium by distance promotion. Consequently, a Cs/Ru molar ratio loading above 0.6, decreases the activity of the Ru/graphitized CNT system.

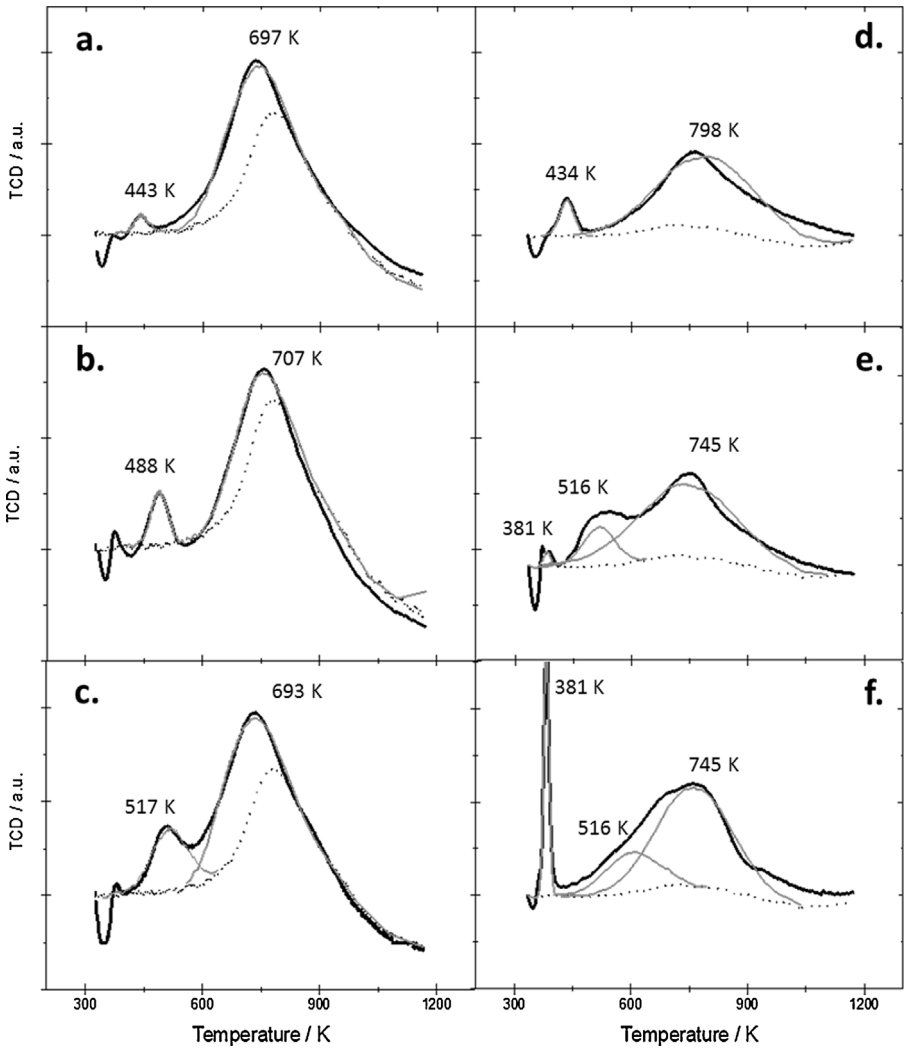

Fig. 8. Temperature programme reduction of (a) 7 wt% Ru/CNT, (b) 7 wt% Ru 4 wt% Cs/CNT, (c) 7 wt% Ru 10 wt% Cs/CNT, (d) 7 wt% Ru/graphitised CNT, (e) 7 wt% Ru 4 wt% Cs/graphitised CNT and (f) 7 wt% Ru 10 wt% Cs/graphitised CNT.

Table 3
Integration of peaks in TPR analyses shown in Fig. 8.

	Catalyst	Peak 1		Peak 2	
		Peak Temp/K	H_2 consumed/mmol g^{-1}	Peak Temp/K	H_2 consumed/mmol g^{-1}
Fig. 4a	7 wt% Ru 0 wt% Cs/commercial CNT	–	–	443	0.0009
Fig. 4b	7 wt% Ru 4 wt% Cs/commercial CNT	–	–	488	0.003
Fig. 4c	7 wt% Ru 10 wt% Cs/commercial CNT	–	–	517	0.008
Fig. 4d	7 wt% Ru 0 wt% Cs/graphitized CNT	–	–	433	0.0019
Fig. 4e	7 wt% Ru 4 wt% Cs/graphitized CNT	378	0.0005	487	0.005
Fig. 4f	7 wt% Ru 10 wt% Cs/graphitized CNT	382	0.0050	517	0.008

4. Conclusions

In ruthenium-based catalysts, a highly conductive support allows the "distance" promotion by electron donating elements such as cesium without blocking the access to the active sites. This synergetic effect facilitates the development of low temperature activity toward ammonia decomposition providing guidelines for further catalyst design and the development of bi-metallic systems. Specifically, core-shell nanoparticles might be capable of intrinsically modifying the ruthenium's electronic properties to reduce the use of this scare and expensive metal or even replace it. The feasibility of ammonia as large-scale hydrogen storage chemical system and its capability of producing hydrogen on-demand at suitable temperatures for fuel cell systems rely on this success.

Acknowledgments

The authors would like to acknowledge the UK Engineering and Physical Science Research Council (grant number EP/K016334/1) for funding, the DTC in the Centre for Sustainable Chemical Technologies (grant number EP/G03768X/1) for AKH's studentship and the Research Catalysis Group at Harwell (RCaH) for access to the TEM microscopy facilities.

References

[1] I.P.o.C. Change, Fifth Assessment report: Climate Change (AR5), 2013.
[2] US Department of Energy Targets for Onboard Hydrogen Storage Systems for Light-Duty Vehicles September, 2009.
[3] A. Klerke, C.H. Christensen, J.K. Norskov, T. Vegge, Ammonia for hydrogen storage: challenges and opportunities, J. Mater. Chem. 18 (2008) 2304–2310.
[4] A. Boisen, S. Dahl, J.K. Norskov, C.H. Christensen, Why the optimal ammonia synthesis catalyst is not the optimal ammonia decomposition catalyst, J. Catal. 230 (2005) 309–312.
[5] M.C.J. Bradford, P.E. Fanning, M.A. Vannice, Kinetics of NH3 decomposition over well dispersed Ru, J. Catal. 172 (1997) 479–484.
[6] F.R. Garcia-Garcia, L. Torrente-Murciano, D. Chadwick, K. Li, Hollow fibre membrane reactors for high H-2 yields in the WGS reaction, J. Membr. Sci. 405 (2012) 30–37.
[7] F. Schuth, R. Palkovits, R. Schlogl, D.S. Su, Ammonia as a possible element in an energy infrastructure: catalysts for ammonia decomposition, Energy Environ. Sci. 5 (2012) 6278–6289.
[8] A. Klerke, S.K. Klitgaard, R. Fehrmann, Catalytic ammonia decomposition over ruthenium nanoparticles supported on nano-titanates, Catal. Lett. 130 (2009) 541–546.
[9] R.Z. Sorensen, A. Klerke, U. Quaade, S. Jensen, O. Hansen, C.H. Christensen, Promoted Ru on high-surface area graphite for efficient miniaturized production of hydrogen from ammonia, Catal. Lett. 112 (2006) 77–81.
[10] A.K. Hill, L. Torrente-Murciano, In-situ H-2 production via low temperature decomposition of ammonia: Insights into the role of cesium as a promoter, Int. J. Hydrog. Energy 39 (2014) 7646–7654.
[11] R. Andrews, D. Jacques, D. Qian, E.C. Dickey, Purification and structural annealing of multiwalled carbon nanotubes at graphitization temperatures, Carbon 39 (2001) 1681–1687.
[12] A.C. Ferrari, J. Robertson, Interpretation of Raman spectra of disordered and amorphous carbon, Phys. Rev. B 61 (2000) 14095–14107.
[13] H.P. Boehm, Surface oxides on carbon and their analysis: a critical assessment, Carbon 40 (2002) 145–149.
[14] F. Rodriguez-Reinoso, The role of carbon materials in heterogeneous catalysis, Carbon 36 (1998) 159–175.
[15] W.Q. Zheng, J. Zhang, B. Zhu, R. Blume, Y.L. Zhang, K. Schlichte, R. Schlogl, F. Schuth, D.S. Su, Structure-function correlations for Ru/CNT in the catalytic decomposition of ammonia, ChemSusChem 3 (2010) 226–230.
[16] J.W. Mintmire, C.T. White, Electronic and structural properties of carbon nanotubes, in: M. Endo, S. Iijima, M.S. Dresselhaus (Eds.), Carbon Nanotubes, Pergamon, Oxford, 1996, pp. 37–46.
[17] D. Mattia, M.P. Rossi, B.M. Kim, G. Korneva, H.H. Bau, Y. Gogotsi, Effect of graphitization on the wettability and electrical conductivity of CVD-carbon nanotubes and films, J. Phys. Chem. B 110 (2006) 9850–9855.
[18] B. Fastrup, On the interaction of N-2 and H-2 with Ru catalyst surfaces, Catal. Lett. 48 (1997) 111–119.